



## Aromatic polyimide foams: factors that lead to high fire performance

M.K. Williams<sup>a,\*</sup>, D.B. Holland<sup>a</sup>, O. Melendez<sup>a</sup>,  
E.S. Weiser<sup>b</sup>, J.R. Brenner<sup>c</sup>, G.L. Nelson<sup>c</sup>

<sup>a</sup>NASA, Testbed Technology, YA-C2-T, Kennedy Space Center, FL 32899, USA

<sup>b</sup>NASA, Mail Stop 226, Langley Research Center, Hampton, VA 23681, USA

<sup>c</sup>Florida Institute of Technology, 150 W. University Blvd., Melbourne, FL 32901, USA

Received 15 September 2003; accepted 15 December 2003

Available online 11 November 2004

### Abstract

In this research, three different, closely related, polyimide foams (namely TEEK-H, TEEK-L, and TEEK-C) were comparatively studied including thermal, mechanical, surface, flammability, and degradation properties. TEEK-H series was the name given to ODDPA/3,4'-ODA (4,4-oxydiphthalic anhydride/3,4-oxydianiline), TEEK-L series for BTDA/4,4'-ODA (3,3,4,4-benzophenone-tetracarboxylic dianhydride/4,4-oxydianiline), and TEEK-CL for BTDA/4,4'-DDSO<sub>2</sub> (3,3,4,4-benzophenone-tetracarboxylic dianhydride/4,4-diaminodiphenyl sulfone). With varying chemistries, densities, and surface areas of these foams, one has the ability to investigate the effects of subtle changes in density, surface area, and chemical structure on fire and thermal properties. Foams have much higher surface areas than solid polymers and are a greater challenge to fire retard [Weiser ES, Johnson TF, St. Clair TL, Echigo Y, Kaneshiro H, Grimsley B, *Journal of High Performance Polymers* 12 (2000) 1–12; Weiser ES, Baillif FF, Grimsley BW, Marchello JM, High temperature structural foam, Proceedings of the 43rd International SAMPE Symposium, May 1998, p. 730–44; Williams MK, et al., In: Nelson GL and Wilkie CA (Eds.), *Fire and polymers: materials and solutions for hazard prevention*, ACS Symposium Series 797, American Chemical Society/Oxford Press, Washington, D.C., 2001, p. 49–62; Williams MK, Nelson GL, Brenner JR, Weiser ES, St. Clair TL, Cell surface area and foam flammability, Proceedings of recent advances in flame retardancy of polymeric materials, 2001]. Detailed fire and thermal properties are discussed.

Published by Elsevier Ltd.

**Keywords:** Polyimide foams; Flammability; Surface area; Fire performance; Thermal properties

### 1. Introduction

Aromatic polyamides have been used for applications in the aerospace and electronic industries. Unique properties, such as thermal and thermo-oxidative stability at elevated temperatures, chemical resistance, and mechanical properties, are common for this class of materials. Newer to the arena of polyimides is the

synthesis of polyimide foams that can be manufactured at densities ranging from 0.008 gm/cc to 0.128 gm/cc and higher. These polyimide foams were developed by NASA Langley Research Center for high-performance applications like the Reusable Launch Vehicle (RLV) program or future generations of launch vehicles. Because of a polyimide's high operating temperature (approximately 260 °C) and cryogenic insulation properties, structural polyimide foams can potentially reduce the amount of Thermal Protection System (TPS) integration structure that is required on an RLV and the total amount of TPS required. A reduction in the TPS

\* Corresponding author.

E-mail addresses: [martha.k.williams@nasa.gov](mailto:martha.k.williams@nasa.gov) (M.K. Williams), [nelson@fit.edu](mailto:nelson@fit.edu) (G.L. Nelson).

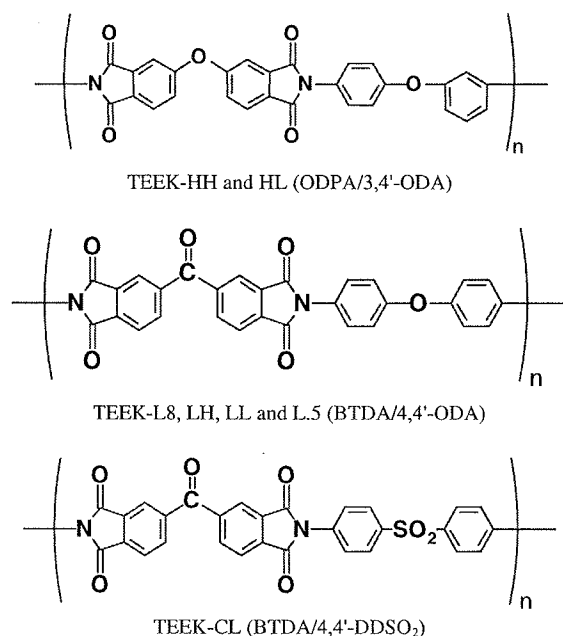


Fig. 1. Chemical structures of foams.

integration structure would reduce the total weight of and cost to build an RLV. This would allow the maximum payload weight to increase and make the vehicle more efficient for commercial applications.

It is essential for the development and application of new materials for next-generation vehicles to understand their fire performance (fire performance is always a significant concern). In this research partnership, three different, closely related polyimide foams were comparatively studied, including thermal, mechanical, surface, flammability, and degradation properties. See Fig. 1 for

Table 1  
Foams, densities, and descriptions

Foam	Density (g/cc)	Description
TEEK-HH	0.082	ODPA/3,4'-ODA (4,4-oxydiphthalic anhydride/3,4-oxydianiline)
TEEK-HL	0.032	ODPA/3,4'-ODA (4,4-oxydiphthalic anhydride/3,4-oxydianiline)
TEEK-L8	0.128	BTDA/4,4'-ODA (3,3,4,4-benzophenone-tetracarboxylic dianhydride/4,4-oxydianiline)
TEEK-LH	0.082	BTDA/4,4'-ODA (3,3,4,4-benzophenone-tetracarboxylic dianhydride/4,4-oxydianiline)
TEEK-LL	0.032	BTDA/4,4'-ODA (3,3,4,4-benzophenone-tetracarboxylic dianhydride/4,4-oxydianiline)
TEEK-L.5	0.008	BTDA/4,4'-ODA (3,3,4,4-benzophenone-tetracarboxylic dianhydride/4,4-oxydianiline)
TEEK-CL	0.032	BTDA/4,4'-DDSO <sub>2</sub> (3,3,4,4-benzophenone-tetracarboxylic dianhydride/4,4-diaminodiphenyl sulfone)

Table 2  
Mechanical properties

Property	TEEK-HH	TEEK-HL	TEEK-LL	TEEK-CL
Tensile strength	1.2 MPa	0.28 MPa	0.26 MPa	0.09 MPa
Tensile strength @ 177 °C	0.81 MPa	0.16 MPa	0.09 MPa	0.05 MPa
Compressive strength @ 10% Defl.	0.84 MPa	0.19 MPa	0.30 MPa	0.098 MPa
Compressive modulus	6.13 MPa	3.89 MPa	11.0 MPa	0.7 MPa
Compressive strength @ 177 °C @ 10% Defl.	0.31 MPa	0.06–0.10 MPa	0.06–0.09 MPa	N/A

structures and Table 1 for chemical names and densities for the materials used. Although polyimide thermal properties have been studied previously, the data relate to films. Because of the larger surface areas of foams, they present a greater challenge to fire retardancy. Understanding degradation and properties such as fire retardancy versus structure (foam versus solid) is fundamental. Subtle differences in chemical structure, varying densities, and cell structure were studied to establish correlations with flame retardancy and thermal stability [3,4].

## 2. Experimental

Foams were synthesized as reported previously [1–2]. Mechanical properties were determined using ASTM D1621-C, D3574, and D638. Tensile and compressive

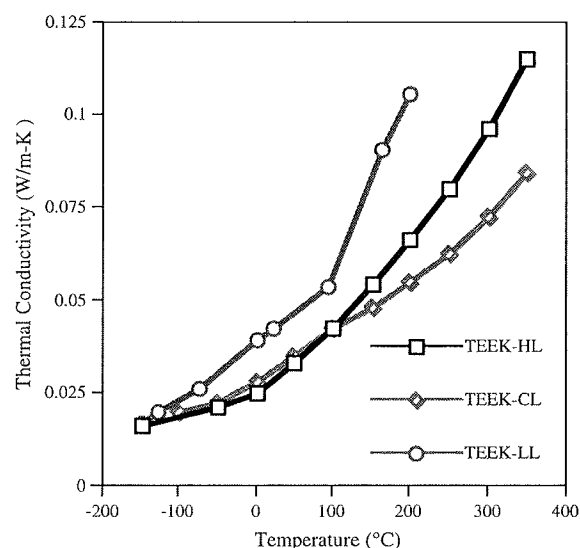


Fig. 2. Thermal conductivity comparison of TEEK foams (0.032 g/cc).

Table 3  
Thermal properties for TEEK polyimide foams

Property	Test method	TEEK-HH	TEEK-HL	TEEK-L8	TEEK-LH	TEEK-LL	TEEK-CL
Density (g/cc)	ASTM D3574 (A)	0.08	0.032	0.128	0.08	0.032	0.032
Thermal stability, loss temp. (°C)	10% wt loss	518	526	522	520	516	528
	50% wt loss	524	522	525	524	524	535
	100% wt loss	580	578	630	627	561	630
Glass transition $T_g$ , temp. (°C)	DSC	237	237	283	278	281	321

strengths at room and elevated temperatures (177 °C) were evaluated using an Instron Tensile Tester, Model 5500R. Adsorption isotherms were measured using a Quantasorb Model QS-17 sorption analyzer and surface areas (porosity) calculated using the BET (after Brunauer, Emmett, and Teller) method [5]. Thermal properties were studied using a TA Instruments Hi-Res Thermometric Analyser Model 2950 and a TA Instruments Dynamic Mechanical Analyser Model 2980. The flammability properties were characterised using ignitability (NASA-STD-6001 and ASTM G72), radiant panel (ASTM E162), oxygen index (ASTM 2863), cone calorimetry (ASTM E1354), glow wire (ASTM D6194) and LOX mechanical impact testing (ASTM D5212). IR microspectroscopy and Raman spectroscopy were dually utilized to study thermal degradation. Oxygen plasma and XPS were used to study atomic oxygen resistance of the foams or degradation due to atomic oxygen exposure [6].

### 3. Results and discussion

Mechanical properties are presented in Table 2. The materials in the TEEK-H series have the highest tensile strengths of the three series and TEEK-L the highest compressive strength and modulus. In Fig. 2 are presented thermal conductivity data for TEEK foams with a density of 0.032 g/cc. As observed, at higher temperatures TEEK-H has the highest thermal conductivity value, with TEEK-C having the better thermal performance. It is to be noted that the difference in thermal conductivity may be attributed to the polymer and the cellular structure (including open or closed cell content) of the foams. Table 3 [3,6] presents thermal analysis data. TEEK-C has a 10 °C higher temperature at 50% weight loss in TGA versus TEEK-L or TEEK-H.  $T_g$ 's are 237 °C for TEEK-H, 281 for TEEK-L and 321 for TEEK-C. Thus TEEK-C clearly has higher thermal properties.

Initial flammability tests showed the foams to be highly flame resistant. Oxygen indices were in the 42–51 range and density dependent. Glow wire testing revealed no ignition and only penetration by the probe, which was also density dependent. Initial radiant panel testing showed the foams with a flame spread index,  $I_s$ , of about 2 [3]. There was, however, sample shrinkage that varied by material and density. The initial round of testing showed that while TEEK-H had better mechanical properties, TEEK-C had higher thermal properties, with TEEK-L in the middle. Thus it was important to understand the three series in detail before a selection of material by application can be made.

While the  $I_s$  in radiant panel was similar for the various foams, there was a factor of more than 4 in shrinkage among the various foam samples (Fig. 3). The initial thought was that shrinkage should follow density.

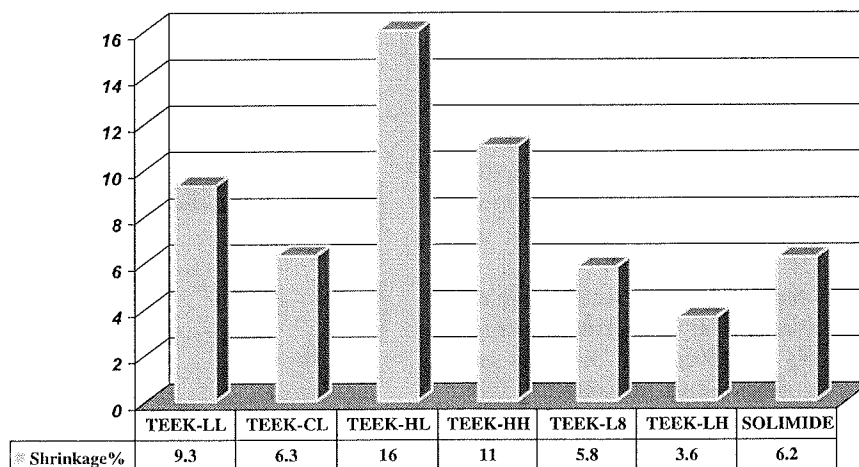


Fig. 3. Shrinkage % for radiant panel samples.

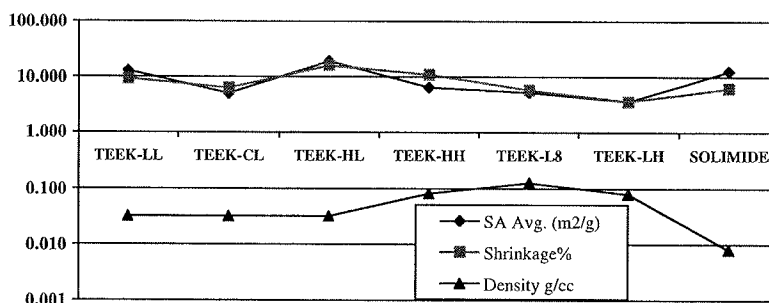


Fig. 4. Comparison of shrinkage %, surface area, and densities.

That proved not to be the case. The opportunity to measure foam surface area presented itself and proved to yield an excellent correlation with sample shrinkage (Fig. 4). Surface area variation over a factor of 5 existed (Table 4) [6]. Materials with the same density had wide differences in surface area and materials with similar surface areas had wide differences in density. Thus both density and surface needed to be studied as other fire and thermal properties were measured.

The radiant panel samples afforded the opportunity to look at mechanisms of degradation. Samples taken 3/6/9 inches from the flame in radiant panel testing were evaluated by infrared. An increase in the OH–NH region versus CH was observed indicating the initial formation of the expected polyamic acid (Table 5 and Fig. 5). TEEK-H showed the largest increase in OH–NH/CH ratio, indicating the highest degree of damage. Raman spectra of samples closest to the radiant panel flame exposure showed formation of a graphite-like structure (e.g., Fig. 6) [6].

Comprehensive cone calorimetry data were obtained on each sample at 50 and 75 kW/m<sup>2</sup> external heat flux. In Table 6 are presented peak heat release data at both fluxes. While foam flammability is usually correlated with density, once again peak rates of heat release did not correlate with density as shown for TEEK-L in Fig. 7. Surface area provided a good qualitative correlation (Fig. 8). In Fig. 9 are presented peak heat release data for foams with similar surface areas. TEEK-H clearly has a higher PHRR, with TEEK-L and TEEK-C ranked similarly. Comparison peak heat release data for same density foams are shown in Fig. 10 [4,6]. Total heat release ought to correlate with density and does as shown in Fig. 11.

Of interest for space applications, the atmosphere at low earth orbit altitudes is essentially opposite to that in the troposphere, 20% N<sub>2</sub> and 80% O<sub>2</sub>. Without an overlying atmosphere to filter short wavelength UV radiation (<243 nm), the molecular oxygen present is largely photo-dissociated to atomic oxygen. Exposure to oxygen plasma is thus another form of radical exposure. The foam samples along with a reference Kapton™ were

Table 4  
TEEK foams, densities, and surface areas

Sample foam	Density (g/cc)	Surface area (m <sup>2</sup> /g)
TEEK-HH	0.08	6.5
TEEK-HL	0.032	19.1
TEEK-L8	0.128	5.2
TEEK-LH	0.08	3.6
TEEK-LL	0.032	12.9
TEEK-L.5	0.008	N/A
TEEK-CL <sup>a</sup>	0.032	5.0
Solimide <sup>®</sup>	0.008	12.6

<sup>a</sup> Notes series with skin.

Table 5  
TEEK-HH, L8, and CL IR OH–NH/CH ratios virgin and post-panel samples, ratio increases and std. deviations

Sample	OH–NH/CH ratio virgin	OH–NH/CH Ratio, 3 inches from radiant panel flame	OH–NH/CH ratio, increase	% Std. dev. virgin	% Std. dev. 3 inches from radiant panel flame
TEEK-HH	1.23	3.10	2.5	5	18
TEEK-L8	2.13	3.39	1.6	5	14
TEEK-CL	3.29	3.85	1.2	6	6

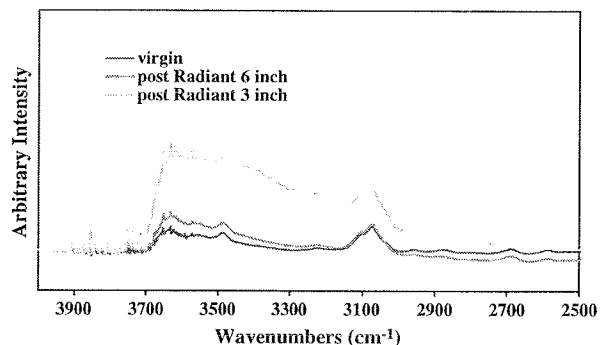


Fig. 5. IR spectra of TEEK-HH at various stages of degradation after radiant panel exposure.

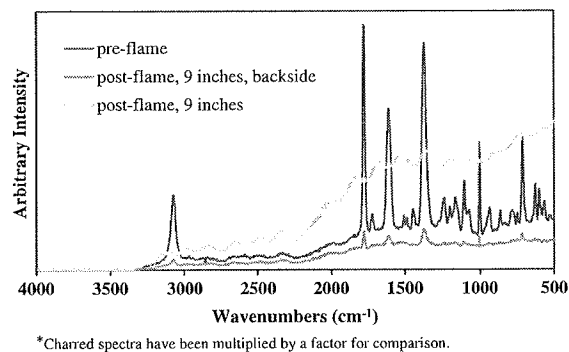


Fig. 6. Raman spectra of TEEK-HH virgin and front and backside 9-inch exposure.

Table 6  
Samples, density, surface area, sample weights, and PHRR data

Sample	Density (g/cc)	Surface area (m <sup>2</sup> /g)	Sample weight (g)	PHRR 75 (kW/m <sup>2</sup> )	Sample weight (g)	PHRR 50 (kW/m <sup>2</sup> )
TEEK-HH	0.08	6.5	19.3 <sup>a</sup>	86 <sup>a</sup>	19.5 <sup>a</sup>	51 <sup>a</sup>
TEEK-HL	0.032	19.1	9.0 <sup>a</sup>	155 <sup>a</sup>	9.1 <sup>a</sup>	60 <sup>a</sup>
TEEK-L8	0.128	5.2	25.8 <sup>a</sup>	55 <sup>a</sup>	25.8 <sup>a</sup>	34 <sup>a</sup>
TEEK-LH	0.08	3.6	20.2 <sup>a</sup>	48 <sup>a</sup>	19.7 <sup>a</sup>	31 <sup>a</sup>
TEEK-LL	0.032	12.9	8.7 <sup>a</sup>	69 <sup>a</sup>	8.9 <sup>a</sup>	43 <sup>a</sup>
TEEK-L.5	0.008	N/A	2.0	45	2.3	26
TEEK-CL <sup>b</sup>	0.032	5.0	8.4	69	7.5	26
TEEK-CLB	0.032	N/A	7.8 <sup>a</sup>	56 <sup>a</sup>	7.8 <sup>a</sup>	45 <sup>a</sup>

<sup>a</sup> Notes average values of two data points.

<sup>b</sup> Notes series with skin.

exposed simultaneously to atomic oxygen at 25% power, the most effective oxygen flux plasma environment (per ASTM E2089-00). Mass loss data versus time for an atomic oxygen flux at 25% power are shown in Fig. 12. Mass loss versus time are similar for TEEK-L and TEEK-C, while TEEK-H shows substantially

higher mass loss versus time. Thus the results are similar to that of cone calorimeter data. Whether mass loss versus time tracks surface area or density is a little too close to call, with data shown in Fig. 13. Upon exposure all four samples showed significant increases in oxygen or overall oxidation with a comparable reduction in carbon, as assessed by XPS high-resolution data, Table 7. The C-1 peak at 284.8 eV results from signals due to C–C, C–N and C–O bonds. The C-2 peak at 288 eV represents the carbonyl group C=O. In the unexposed TEEK-HH virgin sample, the peak shown as C-2 with a binding energy of 286.6 eV is mostly due to the C–O single bond, instead of the C=O. Although there is an overall decrease in carbon, the samples showed a significant increase in C-2 (C=O peak) relative to the peak C-1 with decreasing values in the order TEEK-L > TEEK-H > TEEK-C [7]. The data presented on the lower density HL and LL foams, showing an increase in carbonyl (C=O) after atomic oxygen exposure, correlate with the data previously reported on polyimide films [8,9]. A variation, however, is observed in the higher density TEEK-HH; and a plausible explanation for this decrease in carbonyl from the virgin sample to the exposed sample is the increased density per area of exposure and the extra ether linkage in the TEEK-HH. The C-2 for the carbonyl in the TEEK-HH virgin sample is not distinguishable over that of the C–O–C (dianhydride and diamine) 286 eV peak, and the increase in intensity compared to the other virgin samples is more due to the ether linkage [6].

#### 4. Conclusions

In Table 8, the characteristic properties and performance parameters of the foams are summarised and correlated with chemistry, density, and surface effects.

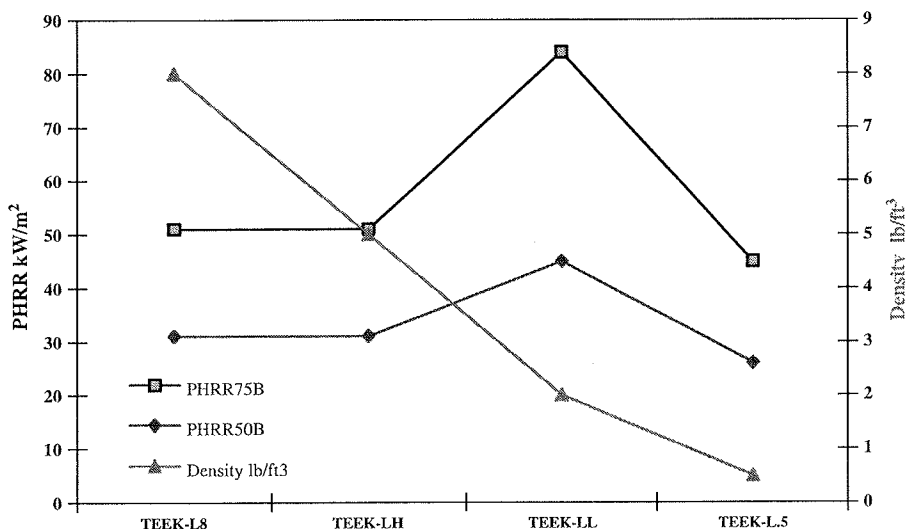


Fig. 7. Same TEEK-L series compared to PHRR at 50 and 70 kW/m<sup>2</sup>.

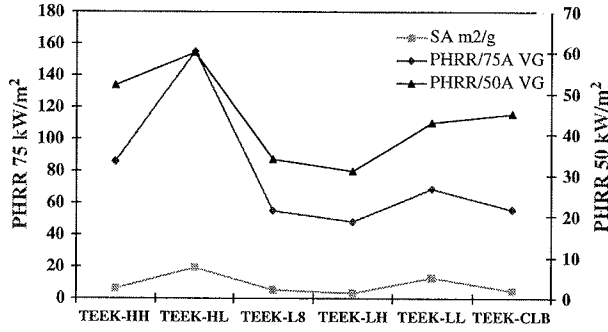


Fig. 8. Foams correlated to PHRR at 50 and 75 kW/m<sup>2</sup> and SA.

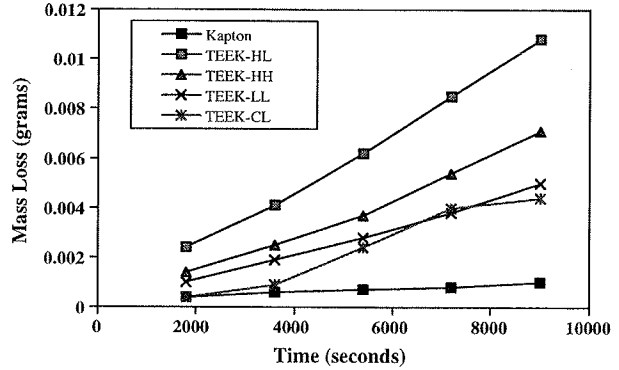


Fig. 12. Mass loss data for HH, HL, LL, CL and Kapton™.

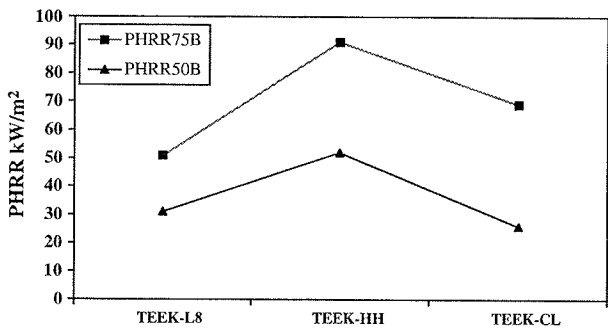


Fig. 9. Foams with different compositions, same SA correlated to PHRR at 50 and 75 kW/m<sup>2</sup>.

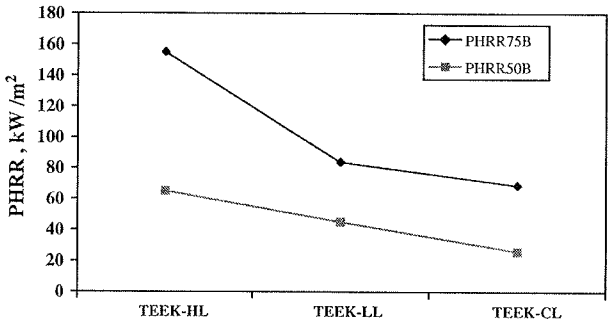


Fig. 10. Same density foams correlated to PHRR at 50 and 70 kW/m<sup>2</sup>.

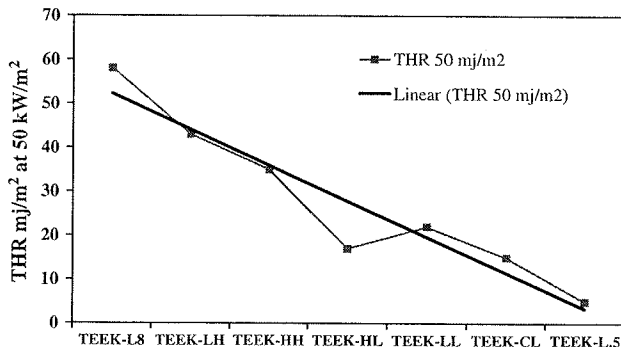


Fig. 11. Comparison of density and THR mJ/m<sup>2</sup> at 50 kW/m<sup>2</sup>.

TEEK-H generally has better mechanical properties than TEEK-L or TEEK-C, with density playing a role. On the other hand, data indicate that density does not appear to have a large effect on the thermal stability of these materials. TEEK-C has the highest degradation temperatures and glass transition temperature. Data presented confirm that these newly developed polyimide foams are all high-performance polymers in their thermal properties. In comparative thermal conductivity data, better thermal performance is observed for TEEK-C having the lowest thermal conductivity value. Their intrinsic flame retardant nature also classifies them as fire resistant polymeric foams (glow wire, OI, and radiant panel data). Because of the intrinsic flame retardant properties of polyimides, this research has given insight into the direct correlation of chemical structure, surface area, and flame retardancy of foams. While subtle changes in chemical structure undoubtedly play a role, radiant panel and cone calorimeter performance indicate that differences in the surface area or cell size of the foams appear to have a large effect on fire performance. Chemical structure, however, may dictate surface area or porosity in the formation of foams. For example, TEEK-CL with its SO<sub>2</sub> linkage, shows the lowest surface area, the lowest peak heat

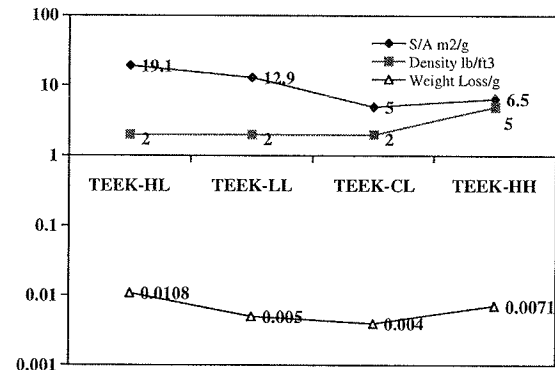


Fig. 13. Correlation of mass loss versus density and surface area.

Table 7  
XPS high-resolution data

Sample I.D.	Carbon					Oxygen				
	Peak	Baseline		After plasma exposure		Peak	Baseline		After plasma exposure	
		BE (eV)	Atomic %	BE (eV)	Atomic %		BE (eV)	Atomic %	BE (eV)	Atomic %
HH	C 1s	284.8	70.1	284.8	55.8	O 1s	533	29.9	532.3	44.3
	C-1	284.6	43.0	284.7	81.3					
	C-2	286.6	57.0	288.7	18.7					
HL	C 1s	284.7	76.5	284.6	48.7	O 1s	532	20.4	532.2	48.7
	C-1	284.7	91.2	284.5	67.8					
	C-2	288.1	8.8	288.0	32.2					
LL	C 1s	284.8	74.0	284.9	56.2	O 1s	532	24	532.7	43.9
	C-1	284.8	92.7	284.7	61.3					
	C-2	288.0	7.2	288.0	38.7					
CL	C 1s	284.8	70.3	284.7	27.8	O 1s	531.7	21.2	532.2	51.9
	C-1	284.9	91.1	284.8	71.4					
	C-2	288.3	8.9	287.9	28.7					

Atomic % does not include nitrogen. C-1 and C-2 represent 100% of C 1s.

release, and highest thermal stability, with the order of thermal stability being TEEK-CL > TEEK-LL > TEEK-HL [4,6]. The thermal degradation appears to follow that observed and reported in film studies, with the chemistry of the diamine the major contributing factor [10].

Data indicate that thermogravimetric analyses (TGA) and differential scanning calorimetry (DSC) analyses can be used to correlate distance from the radiant panel flame to the level of thermal degradation. A Raman study of foam surface degradation showed surface char

formation which appears to be represented in the Raman spectrum by graphite-like structure formation [11]. A definite trend of increased OH–NH/CH ratio in the infrared (IR) was observed, and the OH–NH/CH increase with thermal degradation indicates the formation of a polyamic acid, with the thermal degradation mechanisms similar for all the foams and TEEK-C the most thermally resistant of the foams.

### Acknowledgement

This document was prepared under the sponsorship of the National Aeronautics and Space Administration. Neither the United States Government nor any person acting on behalf of the United States Government assumes any liability resulting from the use of the information contained in this document, or warrants that such use will be free from privately owned rights. The citation of manufacturer's names, trademarks, or other product identification in this document does not constitute an endorsement or approval of the use of such commercial products.

Table 8  
Summary, stability, degradation, and other properties

Property or performance	Sample series, chemistry, density or surface area effects	Reference
Mechanical tensile	H–L > C (somewhat density dependent)	Table 2
Tensile at 177 °C	H > L > C	Table 2
Compressive strength	L > H > C (chemistry > surface area > density dependent)	Table 2
Compressive strength 177 °C	L–H (chemistry, surface area dependent)	Table 2
Glass transition (°C)	C > L > H	Table 3
Thermal conductivity	C > L–H (chemistry dependent, diamine)	Fig. 2
Isothermal TGA	C > L–H (chemistry dependent)	
OI and glow wire	L <sub>better</sub> > H > C (chemistry > surface area > density)	
Radiant panel shrinkage	No precedence within series, surface area dependent	Fig. 4
PHRR same surface area	H <sub>higher</sub> > L–C (surface area dependent)	Fig. 9
Oxygen plasma	C <sub>better</sub> > L > H (chemistry diamine > density–surface area)	Fig. 12

### References

- [1] Weiser ES, Johnson TF, St. Clair TL, Echigo Y, Kaneshiro H, Grimsley B. Journal of High Performance Polymers 2000;12: 1–12.
- [2] Weiser ES, Baillif FF, Grimsley BW, Marchello, JM. High temperature structural foam. In: Proceedings of the 43rd International SAMPE Symposium; May 1998. p. 730–44.
- [3] Williams MK, Nelson GL, Brenner JR, Weiser ES, St. Clair TL. In: Nelson GL, Wilkie CA, editors. Fire and polymers: materials and solutions for hazard prevention. ACS symposium series 797

- Washington, D.C.: American Chemical Society/Oxford Press; 2001. p. 49–62.
- [4] Williams MK, Nelson GL, Brenner JR, Weiser ES, St. Clair, TL. Cell surface area and foam flammability. In: Proceedings of recent advances in flame retardancy of polymeric materials; 2001.
- [5] Gregg SJ, Sing KS. Adsorption, surface area and porosity. New York: Academic Press, Inc; 1982. 303 p.
- [6] Williams MK. A study of the properties of high temperature polyimide foams. Dissertation, Florida Institute of Technology, Melbourne, FL; May 2003.
- [7] Melendez O, Hampton MD, Williams MK, Brown SF, Nelson GL, Weiser ES. Surface evaluation by XPS of high performance polyimide foams. In: AIAA Proceedings, 43rd AIAA/ASME/ASCE/AHS/ASC structures, structural dynamics, and materials conference; 2002.
- [8] Cross JB, Koontz SL, Gregory JC, Edgell MJ. In: Srinivasan V, Banks BA, editors. Hyperthermal Atomic Oxygen Reactions with Kapton and Polyethylene, Materials Degradation in Low Earth Orbit (LEO) 1990. p. 1–13.
- [9] Lu QH, Li M, Zhu Z, Wang Z. Journal of Applied Polymer Science 2001;82:2739–43.
- [10] Cella JA. In: Mittal K, Ghosh M, editors. Degradation and stability of polyimides (polyimides, fundamentals and applications). New York: Marcel Dekker, Inc; 1996. p. 343–65.
- [11] Levchik S, Wilkie CA. In: Grand AF, Wilkie CA, editors. Fire retardancy of polymeric materials. New York: Marcel Dekker; 2000. p. 171–215.